Phase Diagram of Single Crystal MgB_2

G. Karapetrov, U. Welp, A. Rydh, M. Iavarone, W. K. Kwok, G. W. Crabtree, Ch. Marcenat*, L. Paulius,* T. Klein†, J. Marcus,† K. H. P. Kim‡, C. U. Jung‡, H.-S. Lee‡, B. Kang‡, S.-I. Lee‡

Materials Science Division, Argonne National Laboratory, Argonne, Illinois 60439
**Département de Recherche Fondamentale sur la Matière Condensée, Service de Physique, Magnétisme et Superconductivité, CEA-Grenoble, 38054 Grenoble, France*
†Laboratoire d'Etudes des Proprits des Solides, CNRS, BP 166, 38042 Grenoble, France
‡NCRICS and Dept. of Physics, Pohang University of Science and Technology, Pohang 790-784, Republic of Korea

Using magnetization, magneto-transport and single-crystal specific heat measurements we have determined the superconducting phase diagram of MgB_2. The superconducting anisotropy γ changes monotonously from a value of around 2 near T_c to above 4.5 at 22 K. For $H||c$ a pronounced peak effect in the critical current occurs at the upper critical field. We present a strong evidence for a surface superconducting state for $H||c$ which might account for the wide spread in reported values of the superconducting anisotropy γ.

PACS numbers: 74.25.Dw, 74.25.Ha, 74.60.Ec, 74.60.Ge.

1. INTRODUCTION

MgB_2 is an exciting new superconducting material[1] which in addition to its surprisingly high value of T_c displays a variety of unusual properties. Electronic structure calculations[2] indicate a highly anisotropic, complex Fermi surface consisting of two disconnected sections: a three dimensional tubular network of mostly boron π-states and two dimensional cylindrical sheets derived mostly from boron σ-states. Some of these features have been observed in recent de Haas-van Alphen experiments.[3] The appearance of multiple superconducting gaps was predicted,[4] with a large gap resid-

ing on the 2D sheets and a small gap on the 3D network. Specific heat[5] and spectroscopic measurements[6,7] give evidence for this scenario. In addition, calculations within the anisotropic Eliashberg formalism[8] indicate a strongly anisotropic electron-phonon interaction. However, the anisotropy coefficient $\gamma = H_{c2}^{ab}/H_{c2}^{c} = \xi_{ab}/\xi_c$, is not well established for MgB_2. Here, H_{c2}^{ab}, H_{c2}^{c}, ξ_{ab} and ξ_c are the in-plane and out-of-plane upper critical fields and Ginsburg-Landau coherence lengths, respectively. Reported values vary widely ranging from 1.1 to 6 depending on the measurement technique and on samples type, i.e. single crystals,[9–14] oriented films,[15] aligned crystallites,[16] or powders.[17,18] Recent torque[13] and thermal conductivity[14] measurements on single crystals as well as magnetization measurements on powders[18] indicate that the anisotropy coefficient is temperature dependent, increasing strongly with decreasing temperature.

In this paper we present a detailed study of the superconducting phase diagram of MgB_2 by combining magnetization $M(T)$, magneto-transport, and single-crystal specific heat $C_p(T)$ measurements on same single crystals. The upper critical fields for in- and out-of-plane fields were determined from $M(T)$ and $C_p(T)$ data yielding a coherence length of ξ_{ab} (0) = 9.4 nm. Transport data reveal a pronounced peak-effect in the critical current density at H_{c2}^{c}. For fields above H_{c2}^{c}, extending to approximately $1.7\times H_{c2}^{c}$, we observe strongly non-ohmic transport behavior which we attribute to surface superconductivity. The upward curvature in H_{c2}^{ab}(T) results in a temperature dependent anisotropy that increases from about 2 near T_c to above 4.5 at 22 K. We note that the occurrence of surface superconductivity could account for the wide variation in reported values for the anisotropy constant.

2. MgB_2 SAMPLES

The MgB_2 crystals were prepared by heat-treating a 1:1 mixture of Mg and B under high pressure conditions.[19] The crystals are well shaped with straight hexagonal facets and smooth faces (see picture in inset of Fig. 1b) with typical size of 50 μm. The magnetization was measured in a commercial SQUID magnetometer. The specific heat measurements were performed using an ac-specific heat calorimeter[20] optimized to detect signals from minute samples (on the order of 50 ng).

3. EXPERIMENT

Temperature dependent magnetization measurements $M(T)$ (Fig.1a) were performed on warming after field cooling the sample in $H||c$. Breaks in the slope of the temperature dependence of the magnetization indicated by

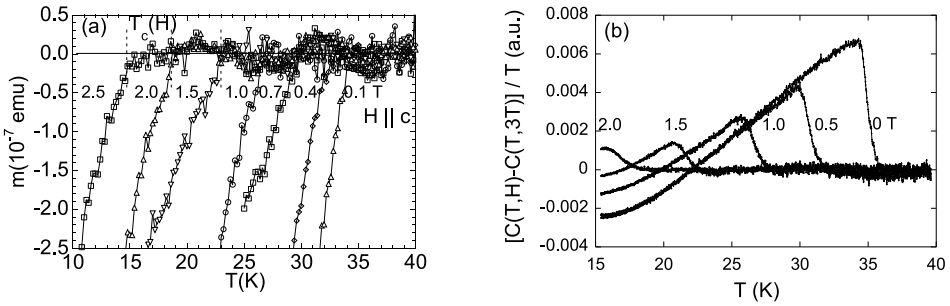

Fig. 1. a) Temperature dependence of the diamagnetic moment of MgB_2 single crystal measured on warming after cooling in the indicated fields parallel c axis; b) Temperature dependence of the heat capacity in magnetic field parallel to the c-axis. Data obtained in H=3T was used to subtract the background signal.

the vertical dotted lines are clearly seen and mark the onset of superconductivity. With increasing field there is an essentially parallel shift of the $M(T)$ curve to lower temperatures. This shift is much more pronounced for $H||c$ indicating a strong superconducting anisotropy of MgB_2 as discussed below. Figure 1b shows the temperature dependence of the heat capacity. In zero field a clear step in the $C_p(T)$ with a width of about 2 K is observed. With increasing field the step stays well defined and the step height decreases as expected. However, in contrast to results on polycrystalline samples,[5] the width remains essentially constant. A phase boundary in H-T space was obtained by defining T_c using an entropy conserving construction.[20] This phase line agrees well with that determined from $M(T)$ as discussed below. Thus, the data shown in Fig. 1 represent the thermodynamic bulk transition of MgB_2 into the superconducting state.

The magneto-resistive transitions with the field along the c-axis are shown in Figure 2a. The sample is characterized by a resistivity of ρ =1.6 $\mu\Omega$cm at 40 K and a negligibly small normal state magneto-resistance. With increasing field the resistive transition moves to lower temperature and broadens significantly. Similar broadening has been observed in previous studies on single crystals.[10,11] However, here we show that the broadening is strongly current dependent. Non-ohmic behavior appears early at the onset of the superconducting transition. With increasing current a steep resistive drop emerges at a lower almost current independent temperature. At even higher currents a non-monotonic, hysteretic resistivity behavior arises that is reminiscent of the peak-effect. Peak-effects, that is, sharp maxima in the temperature and/or field dependence (Fig.2b) of the critical current

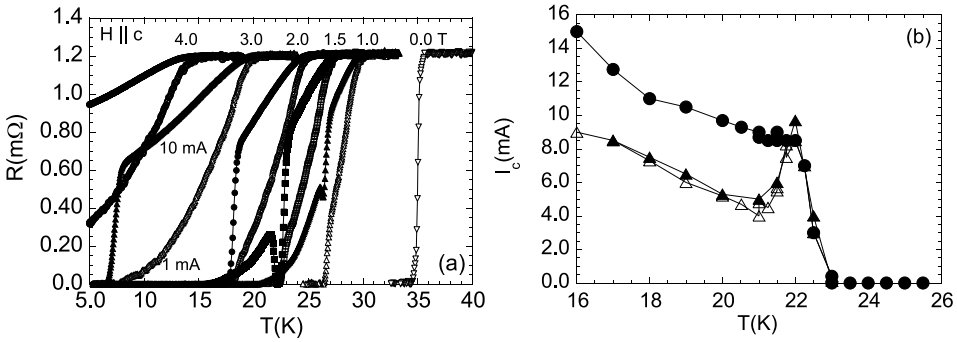

Fig. 2. a) Resistive transition measured on cooling in various fields and at different current densities. 1 mA corresponds to a current density of 360A/cm^2; b) Temperature dependence of the critical current in 1.5 T showing the peak effect

and the corresponding suppression of the resistivity, have been observed just below the $H_{c2}(T)$ in a variety of low-pinning superconductors, including $NbSe_2$,[21,22] Nb[23] and borocarbides.[24] For fields applied along the ab-directions the resistive transitions in magnetic fields do not broaden in agreement with previous reports,[10,11] and the peak-effect is largely suppressed.

The peak-effect region is accompanied with peculiar I-V characteristics like those shown in Fig.3 at 1.5 T || c. The current-voltage (I-V) characteristics after field-cooling to 20 K display pronounced hysteretic behavior. On first increasing the current, a sharp onset of dissipation occurs near a critical current of 10 mA whereas for decreasing current zero-dissipation is approached near 5.5 mA. All subsequent current ramps and also the $I-V$s taken after zero-field cooling follow this curve. These results are a manifestation of a current induced transition from a meta-stable high-I_c vortex phase into a stable low-I_c phase. As the sample is field cooled through $T_{c2}(H)$ a high-pinning vortex phase nucleates and stays in thermodynamic equilibrium until the peak-effect temperature is reached (Fig.2b). At lower temperatures this phase may survive as supercooled meta-stable state. The application of a strong enough current dislodges vortices from their pinned meta-stable configuration and triggers a transition into the stable low-pinning state which does not change on subsequent current ramps. In zero-field cooled measurements the initial vortex configuration is the result of flux-gradient driven motion of vortices across the sample and a low-pinning state analogous to the current-induced state is created. Consequently, the zero-field cooled I-V coincides with the stable field-cooled I-V. Similar results have recently been reported for $NbSe_2$[22] when fast current ramps are applied.

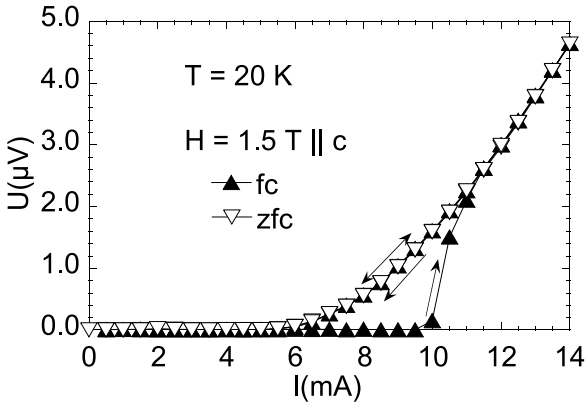

Fig. 3. Hysteretic I-V characteristics at 20 K and 1.5 T || c measured for increasing and decreasing current after field cooling and after zero-field cooling.

4. DISCUSSION

Summary of the magnetic, calorimetric and transport data is in the phase diagram shown in Fig. 4a. For $H||c$ the onsets of superconductivity as determined from $M(T)$ and $C_p(T)$ coincide with each other and with the location of the peak effect within the experimental uncertainty. This line is identified with the upper critical field for the c-axis, $H_{c2}^c(T)$. A zero-temperature value of $H_{c2}^c(0) \approx 3.5$ T can be estimated which, using the relation $H_{c2}^c(0) = \Phi_0/2\pi{\xi_{ab}}^2(0)$, yields the zero-temperature coherence length $\xi_{ab}(0) \approx 9.4$ nm.

Phase diagram in Figure 4a shows that the onset of non-ohmic transport with decreasing temperature defines a line in the phase diagram lying by a factor 1.66 above the H_{c2}^c -line. This suggests that the resistive onset is a manifestation of surface superconductivity[25] at H_{c3} which for a flat surface in parallel magnetic field occurs at $1.7\times\mathrm{H}_{c2}$. For $H||c$ the surface-superconducting currents are flowing on the vertical side faces of the plate-like crystals. Although resistive transitions as shown in Fig. 2a could in principle result from filamentary conduction along impurity phases the observation of a single sharp, current-independent superconducting transition in zero field indicates an intrinsic mechanism. Within the experimental resolution there is no feature in the magnetization and specific heat data that would indicate a second superconducting phase. Furthermore, non-ohmic transport data above the bulk upper critical field have been reported for NbTa and PbIn samples[26] and for $NbSe_2$ crystals .[27] These results, closely resembling those in Fig. 2a, have been interpreted as signature of surface

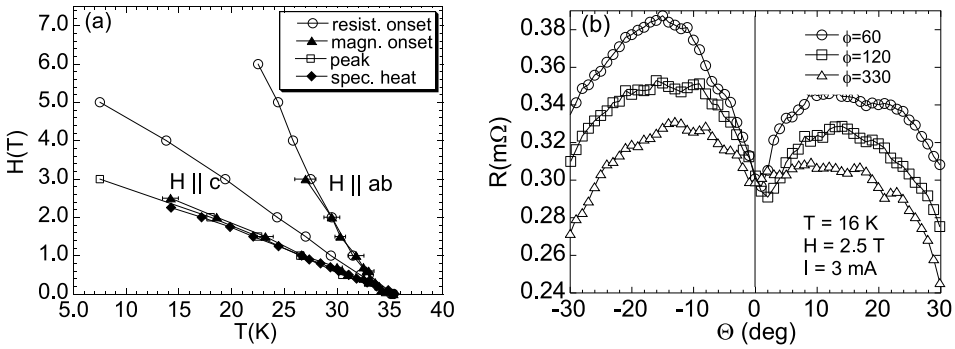

Fig. 4. a) H-T phase diagram of MgB_2 as determined from the magnetization, specific heat, and transport measurements; b) Angular dependence of the resitivity. The corners of the crystal make angles of 60° and 120°. Θ is the polar angle with respect to the c-axis and ϕ is the azimuthal angle with respect to the net current direction. For $\phi = 60°$ the applied field rotates in a plane perpendicular to the side face, for $\phi = -30°$ the field rotates almost in the side face.

superconductivity.

The angular dependence of the resistivity of a third crystal measured in the regime of non-ohmic transport above the bulk upper critical field is shown in Fig. 4b. Pronounced cusp-like dips in the resistance with a width of about 5° are observed when the field is aligned with the c-axis. With increasing angle Θ the resistance increases rapidly and at high angles decreases again due to the superconducting anisotropy of MgB_2. This kind of angular dependence could be caused by extended crystal defects containing the c-axis such as small angle grain boundaries. However, x-ray diffraction reveals a very high quality of the crystals without any indication for this type of defects.[19] Furthermore, the dip is strongly dependent on the azimuthal angle being most pronounced when the field rotates in a plane perpendicular to the side face ($\phi = 60°$) and being largely suppressed for rotation in the plane of the side face ($\phi = -30°$). These results are consistent with a surface superconducting state which is rapidly suppressed by magnetic field components perpendicular to the surface.[28]

Since surface superconductivity does not contribute to the magnetization[25] nor the thermal conductivity of macroscopic samples but does induce non-linear response in the resistivity, a discrepancy between determinations of anisotropy constant might be expected when measuring with different methods.Reported γ-values determined from resistivity measurements (usually the resistive onset is identified with H_{c2}) on crystals[9–12] as well as on c-axis oriented films[15] are generally low, in the range of 2 to 3. In contrast,

magnetic measurements on either powder samples[17,18] or on single crystals[13] as well as thermal conductivity measurements[14] yield γ-values around 6 at low temperatures.

While the upper critical field for $H||c$ follows a conventional temperature dependence, a pronounced upward curvature of $H_{c2}^{ab}(T)$ was observed. As a result the superconducting anisotropy is temperature dependent. Similar results have recently been obtained from torque ,[13] magnetization on powder samples [18] and thermal conductivity [14] measurements. At high temperatures (i.e. low fields) γ has a value between 1.5 and 2, and reaches values above 4.5 near 22 K. An upward curvature of the $H_{c2}(T)$-line can arise in clean superconductors due to non-local effects as seen for example in borocarbides.[29] However, in those materials the upward curvature occurs in all crystal directions, and the out-of-plane anisotropy is essentially temperature independent. An alternative origin of the temperature dependent anisotropy could lie in the two-gap structure of MgB_2. Since the small 3D gap is readily suppressed in applied fields[5,6] MgB_2 behaves like a quasi 2D superconductor in sufficiently high fields parallel fields. Thus, a steep H_{c2}^{ab}-line can be expected. The cross-over between predominantly 3D to 2D behavior occurs around 0.5 T. Spectroscopic[6] as well as specific heat measurements[5] indicate that the 3D gap is suppressed in a similar field range.

5. CONCLUSIONS

In conclusion, the superconducting phase diagram of MgB_2 has been determined using magnetization, magneto-transport and the first single-crystal specific heat measurements. The in-plane coherence length is 9.4 nm corresponding to $H_{c2}^{c}(0) \approx 3.5$ T. The superconducting anisotropy increases with decreasing temperature from a value around 2 near T_c to above 4.5 at 22 K. For $H||c$ a pronounced peak effect in the critical current occurs at the upper critical field. Evidence for a surface superconducting state is presented for $H||c$ which might account for the wide spread of reported values for the anisotropy coefficient.

ACKNOWLEDGMENTS

This work was supported by the U.S. Department of Energy, BES, Materials Science under contract W-31-109-ENG-38, by the National Science Foundation under grant No.0072880, the Fulbright Fellowship (A.R.), and by the Ministry of Science and Technology of Korea through the Creative Research Initiative Program.

REFERENCES

1. J. Nagamatsu et al., Nature **410**, 63 (2001).
2. J. M. An, W. E. Pickett, Phys. Rev. Lett. **86**, 4366 (2001); J. Kortus et al., Phys. Rev. Lett. **86**, 4656 (2001).
3. E. A. Yelland et al., Phys. Rev. Lett. **88**, 217002 (2002).
4. A. Y. Liu et al., Phys. Rev. Lett. **87**, 087005 (2001).
5. F. Bouquet et al., Phys. Rev. Lett. **87**, 047001 (2001); Y. Wang et al., Physica **355C**, 179 (2001).
6. P. Szabo et al., Phys. Rev. Lett. **87**, 137005 (2001).
7. F.Giubileo et al., Phys. Rev. Lett. **87**, 177008 (2001); X. K. Chen et al., Phys. Rev. Lett. **87**, 157002 (2001); H. Schmidt et al., Phys. Rev. Lett. **88**, 127002 (2002); M. Iavarone et al., cond-mat/0203329.
8. H. J. Choi et al., cond-mat/0111182; *ibid.* cond-mat/0111183.
9. K. H. P. Kim et al., Phys. Rev. B **65**, 100510 (2002).
10. S. Lee et al., J. Phys. Soc. Jpn. **70**, 2255 (2001); Yu. Eltsev et al., cond-mat/0202133; Phys. Rev. B **65**, 140501 (2002).
11. A. K. Pradhan et al., Phys. Rev. B **64**, 212509 (2001).
12. M. Xu et al., Appl. Phys. Lett. **79**, 2779 (2001).
13. M. Angst et al., Phys. Rev. Lett. **88**, 167004 (2002).
14. A. V. Sologubenko et al., Phys. Rev. B **65**, 180505 (2002).
15. S. Patnaik et al., Supercond. Sci. Techn. **14**, 315 (2001); M. H. Jung et al., Chem. Phys. Lett. **343**, 447 (2001); R. J. Olsson et al., cond-mat/0201022.
16. O. F. de Lima et al. Phys. Rev. Lett. **86**, 5974 (2001).
17. F. Simon et al., Phys. Rev. Lett. **87**, 047002 (2001); S. L. Bud'ko et al., Phys. Rev. B **64**, 180506 (2001).
18. S. L. Bud'ko et al., cond-mat/0201085.
19. C. U. Jung et al., cond-mat/0203123.
20. F. Bouquet et al., Nature **411**, 448 (2001).
21. M. Higgins, S. Bhattacharya, Physica C **257**, 232 (1996); X. S. Ling et al., Phys. Rev. B **57**, 3249 (1998); Y. Paltiel et al., Phys. Rev. Lett. **85**, 3712 (2000).
22. Z. L. Xiao et al., Phys. Rev. Lett. **85**, 3265 (2000).
23. P. L. Gammel et al., Phys. Rev. Lett. **80**, 833 (1998); X. S. Ling et al., Phys. Rev. Lett. **86**, 712 (2001); W. deSorbo, Rev. Mod. Phys. **36** 90 (1964).
24. K. J. Song et al., Phys. Rev. B **59**, 6620 (1999); S. S. James et al., Physica C **332**, 173 (2000).
25. D. Saint-James and P. G. de Gennes, Phys. Lett. **7**, 306 (1963); A. A. Abrikosov, Sov. Phys.-JETP **20**, 480 (1965).
26. C. F. Hempstead, Y. B. Kim, Phys. Rev. Lett. **12**, 145 (1964).
27. G. D'Anna et al., Phys. Rev. B **54**, 6583 (1996).
28. R. S. Thompson, Sov. Phys.-JETP **42**, 1144 (1976).
29. V. Metlushko et al., Phys. Rev. Lett. **79**, 1738 (1997).